

Short term power forecasts for large offshore wind turbine arrays

Problem presented by

Jeremy Parkes

GL Garad Hassan

Executive Summary

Methods are presented for precise prediction of windspeeds at a wind-farm using a combination of numerical weather prediction models and on-site wind speed measurements. Simple techniques are used to investigate the properties of the data. More advanced techniques are tested for the predictive value in forecasting including techniques from *autoregressive models*, *data assimilation*, *artificial neural networks* and *kernel dressing*. The performance of the resulting forecasts are compared with the measured wind speeds using a range of forecast windows.

Version 1.0

October 24, 2013

iii+26 pages

Report author

Oscar Benjamin, Petros Mina, László Arany, Colm Connaughton, Sam Cox,
Milena Kresoja, Abhishek Shukla, Ed Wheatcroft, James Tull, Samuel Groth,
Siân Jenkins, Chris Budd, Leonard Smith

Contributors

Oscar Benjamin (University of Bristol),
Petros Mina (University of Bristol),
László Arany (University of Bristol),
Colm Connaughton (University of Warwick),
Sam Cox (University of Leicester),
Milena Kresoja (University of Novi Sad),
Abhishek Shukla (University of Warwick),
Ed Wheatcroft (London School of Economics),
James Tull (Imperial College),
Samuel Groth (University of Reading),
Siân Jenkins (University of Bath),
Chris Budd (University of Bath),
Leonard Smith (London School of Economics)

ESGI91 was jointly organised by

University of Bristol
Knowledge Transfer Network for Industrial Mathematics

and was supported by

Natural Environment Research Council
Oxford Centre for Collaborative Applied Mathematics
Warwick Complexity Centre

Contents

1	Introduction	1
2	Instantaneous linear prediction	4
3	Auto-regressive models	6
4	4D-Var Data assimilation	10
5	Artificial neural networks	15
5.1	Generalised Regression Neural Networks	15
5.2	ANN prediction from SCADA data	16
5.3	ANN prediction from Numerical Weather Prediction data	18
5.4	Remarks and possible future work	19
6	Kernel dressing	20
6.1	Running mean and variance normal distribution model	23
6.2	Individual Kernel Dressed Model forecasts	24
6.3	Possible future work	25
7	Conclusions	25
	Bibliography	26

1 Introduction

- (1.1) Onshore and offshore windfarms are increasingly being used for power generation both in the UK and globally. Since power generation from windfarms is intermittent, a reliable electricity supply must use windfarms in combinations with other energy sources. It is only possible to make use of the energy from windfarms by producing less energy from other energy sources if the output can be reliably predicted in advance. Since the most significant factor determining the power generation of a windfarm is wind speed accurate forecasts of this are essential. However, wind speed can change dramatically on a timescale of hours. Figure 1 shows recordings of wind speeds from an offshore windfarm.

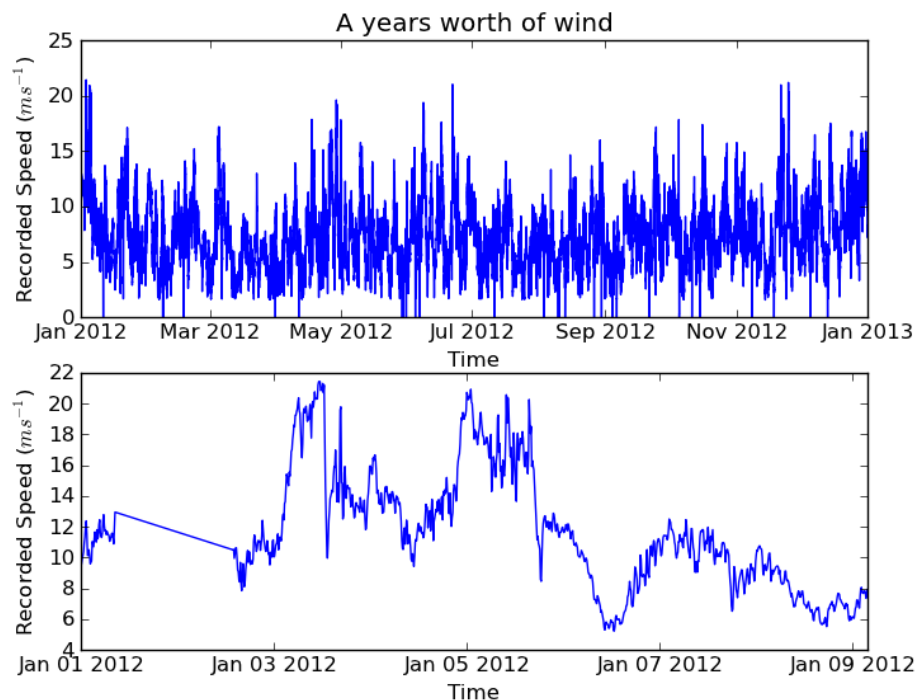


Figure 1: Measured wind speeds at an offshore windfarm at different timescales. The top panel shows wind speed measurements over a whole year. The bottom panel shows wind speed measurements over the first week of the year. The long straight line from 1st-2nd Jan is a period during which no measurement data is available.

- (1.2) GL Garrad Hassan (GH) provides a continuous real-time forecasting service to operators of windfarms providing accurate predictions of wind speed and

power output for individual windfarms from 0-48 hours in advance. The forecasting service makes predictions based on numerical weather prediction (NWP) models and onsite wind measurements (known as SCADA). The NWP and SCADA data are combined to produce estimates of future windspeed with a root mean squared (RMS) error ranging from around 2% (1 hour in advance) to around 6% (48 hours in advance).

- (1.3) NWP models are macroscale numerical simulations of atmospheric dynamics used for weather forecasting in general. Different NWP models are more accurate for predicting the weather under different situations. Forecasters using NWP models will release predictions of the weather for up to two weeks in advance and update their prediction every 3-12 hours. Each forecast gives a prediction of the weather for each hour over the subsequent 1-2 weeks. NWP models describe the atmosphere in terms of finite elements where the size of each element is on the order of kilometres. GH uses interpolation to convert this to an estimate of the weather at the site of the windfarm. Figure 2 shows how the forecast estimate at different times in advance correlates with the recorded windspeed for different NWP models for a specific windfarm. The correlation for the NWP models ranges from around 0.9 for forecasting (or estimating) the windspeed at the current time to around 0.7-0.8 for forecasting 48 hours ahead.
- (1.4) SCADA data recording the actual windspeed at windfarms is available to GH in real time. Every 10 minutes an average wind speed and direction measurement is received by GH. This reading is based on the previous 10 minutes before the measurement is received. This data is used both to make a forecast and also to validate forecasts retrospectively. Figure 2 shows that the correlation between the SCADA windspeed data and its own value at a later time is higher when compared to the correlation between the NWP forecast and the actual wind speed over a 0-3 hours window. This suggests that at very short times the best prediction of the windspeed should be based strongly on the SCADA data. However, when forecasting more than 10 hours ahead the SCADA data has a much lower correlation than any of the NWP models, so the NWP data will likely have more predictive value in this window.
- (1.5) GH combines the NWP and SCADA data to provide realtime forecasting.

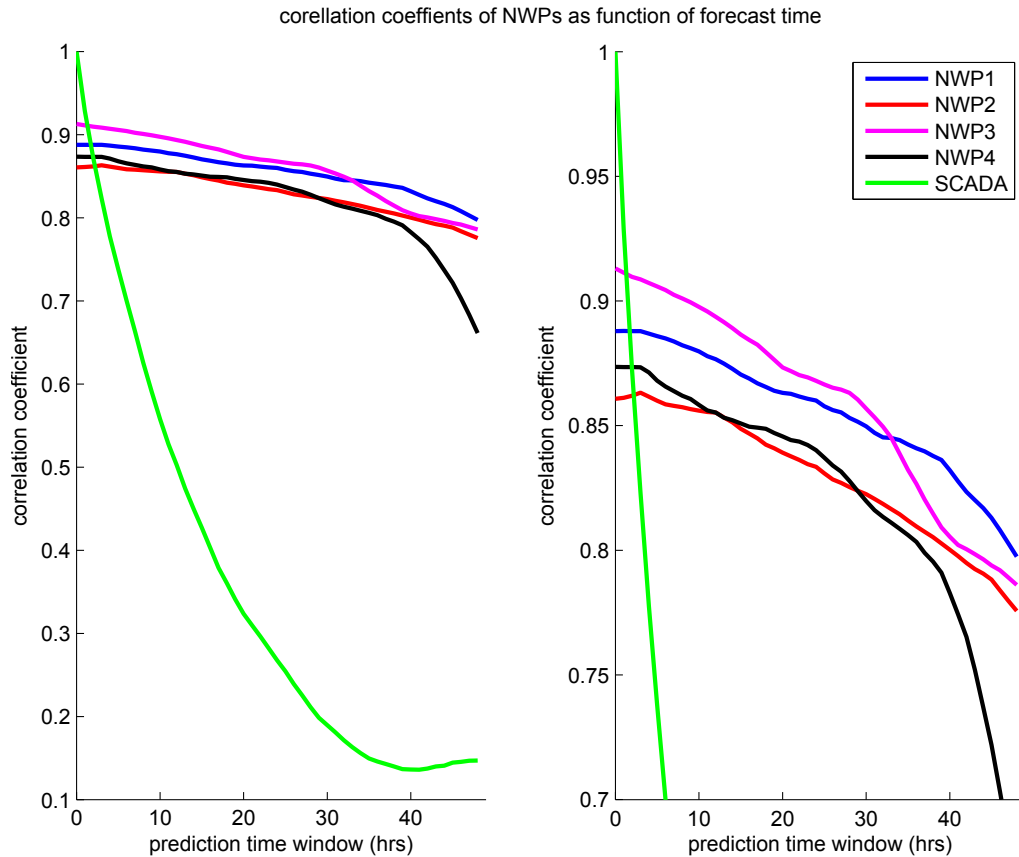


Figure 2: Correlation between NWP estimates of the wind speed and NWP predictions as a function of prediction time window. The prediction time window is the the number of hours in advance that a forecast is made for the wind speed. For this windfarm there are 4 different NWP models available giving different predictions. Also shown is the autocorrelation of the measured windspeeds (SCADA). The panel on the right shows a zoom view of the panel on the left to better illustrate the differences between the NWP models. The SCADA data gives a higher correlation for time windows less than 2 hours but correlates significantly less well than all of the NWP predictions at windows of more than around 4 hours.

They have combined a number of techniques for extracting an improved forecast of weather at the site of the windfarm based on the NWP and SCADA data available. The aim of the study group was to investigate the scope for using novel techniques not employed by GH in the area of windspeed prediction. The study group has investigated the data, applied a number of different techniques for combining the data sources, and attempted to evaluate their applicability. In the following sections each method and the available results are described, starting with the simplest that we use as

benchmarks.

2 Instantaneous linear prediction

- (2.1) Linear regression analysis is perhaps the most simple form of bias correction. The aim is to eradicate some of the systematic error in the different forecasts by first assuming (slightly naïvely) that the error in the windspeed forecast is linear. This systematic error can be seen in figure 3. Each of the NWP models obtains approximately the correct distribution of windspeeds throughout the year when compared with the measured data, however they are all approximately shifted somewhat.

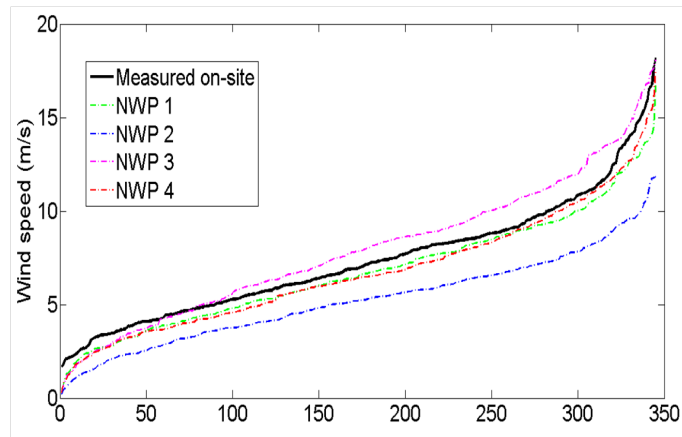


Figure 3: Forecast windspeed by the 4 different NWP models one day in advance compared with the on-site measured windspeeds for all days (for which there is data) in 2012. For visual clarity the days (x -axis) have been reordered to produce a plot where the windspeed is monotonically increasing.

- (2.2) We can calculate the shift by simply computing the least squares fit of each NWP output to the measured data. The shifted NWPs are shown in figure 4. The process of least squares fitting will be elaborated upon below.
- (2.3) A slightly different approach is to combine the four different forecasts in such a way as to obtain a forecast superior to each of the individual NWP models. This is done by taking a linear combination of the output of the four NWPs, that is, we write:

$$\tilde{NWP} = w_1 NWP_1 + w_2 NWP_2 + w_3 NWP_3 + w_4 NWP_4. \quad (2.1)$$

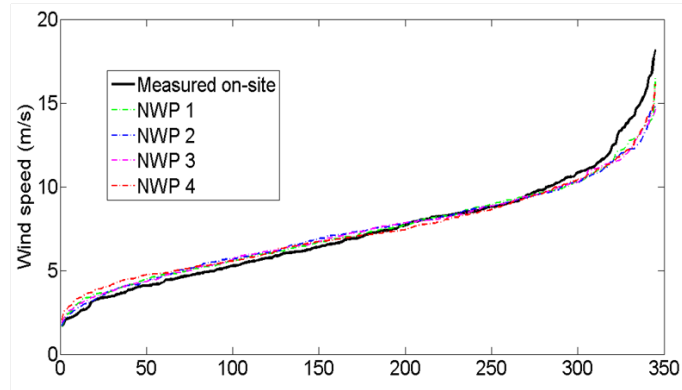


Figure 4: Forecast windspeed of the 4 different NWP models presented in figure 3 after the bias is corrected for, alongside on-site measured data.

In order to determine weights w_i for $i = 1, \dots, 4$ we compute the discrete least squares fit to the SCADA measurements. This is done by assembling the overdetermined system of equations:

$$\begin{pmatrix} \uparrow & \uparrow & \uparrow & \uparrow \\ NWP_1 & NWP_2 & NWP_3 & NWP_4 \\ \downarrow & \downarrow & \downarrow & \downarrow \end{pmatrix} \begin{pmatrix} w_1 \\ w_2 \\ w_3 \\ w_4 \end{pmatrix} = \begin{pmatrix} \uparrow \\ SCADA \\ \downarrow \end{pmatrix}, \quad (2.2)$$

and find numerical values for the coefficients w_i for $i = 1, \dots, 4$ which minimise the function ϵ defined as:

$$\epsilon(\mathbf{w}) = \|\mathbf{b} - \mathbf{A}\mathbf{w}\|_{l^2}^2,$$

where:

$$\mathbf{A} = \begin{pmatrix} \uparrow & \uparrow & \uparrow & \uparrow \\ NWP_1 & NWP_2 & NWP_3 & NWP_4 \\ \downarrow & \downarrow & \downarrow & \downarrow \end{pmatrix},$$

$$\mathbf{w} = \begin{pmatrix} w_1 \\ w_2 \\ w_3 \\ w_4 \end{pmatrix},$$

-	NWP 1	NWP 2	NWP 3	NWP 4	\tilde{NWP}
RMS error, 48 hour	1.84	1.92	1.82	2.23	1.68
RMS error, 30 hour	1.63	1.73	1.59	1.77	1.46
RMS error, 4 hour	1.49	1.52	1.28	1.58	1.28

Table 1: RMS errors for each of the NWP models as well as the optimally weighted average of the four. The errors are shown for three different forecast windows, namely 4, 30 and 48 hours.

$$\mathbf{b} = \begin{pmatrix} \uparrow \\ SCADA \\ \downarrow \end{pmatrix}.$$

This is achieved simply by attempting to solve the above system as one would do with a standard solvable system of equations, using backslash in Matlab for example.

- (2.4) We performed this fit using the forecast and SCADA data for the first half of 2012 and then used the calculated weights to forecast the wind using the \tilde{NWP} for the second half of the year. This was done for 3 different forecasting windows, namely 4 hour, 30 hour and 48 hour time windows and the resulting error in the optimised forecast has been compared to that achieved using any of the individual NWP model forecasts. The results for 4 hour and 48 hour forecasts are shown in figure 5. The optimal weighting minimises the RMS error and outperforms any individual NWP for both 4 and 48 hour forecast horizons and, as can be seen in Table 1 below. The improvement over each the individual forecasts appears to increase the longer the forecasting window.

3 Auto-regressive models

- (3.1) The SCADA data from Windfarm 4 was first cleaned up by removing any zero values of the velocity and converting the calendar dates into absolute time units measured in days starting from the beginning of the data set (day zero). The data were then linearly interpolated, the mean-subtracted and resampled at regular 10 minute intervals. This produced a uniformly sampled, mean-zero timeseries, (t_i, v_i) , $i = 1 \dots N$, without gaps or zeroes.
- (3.2) Smoothed timeseries were produced by filtering the data with a moving

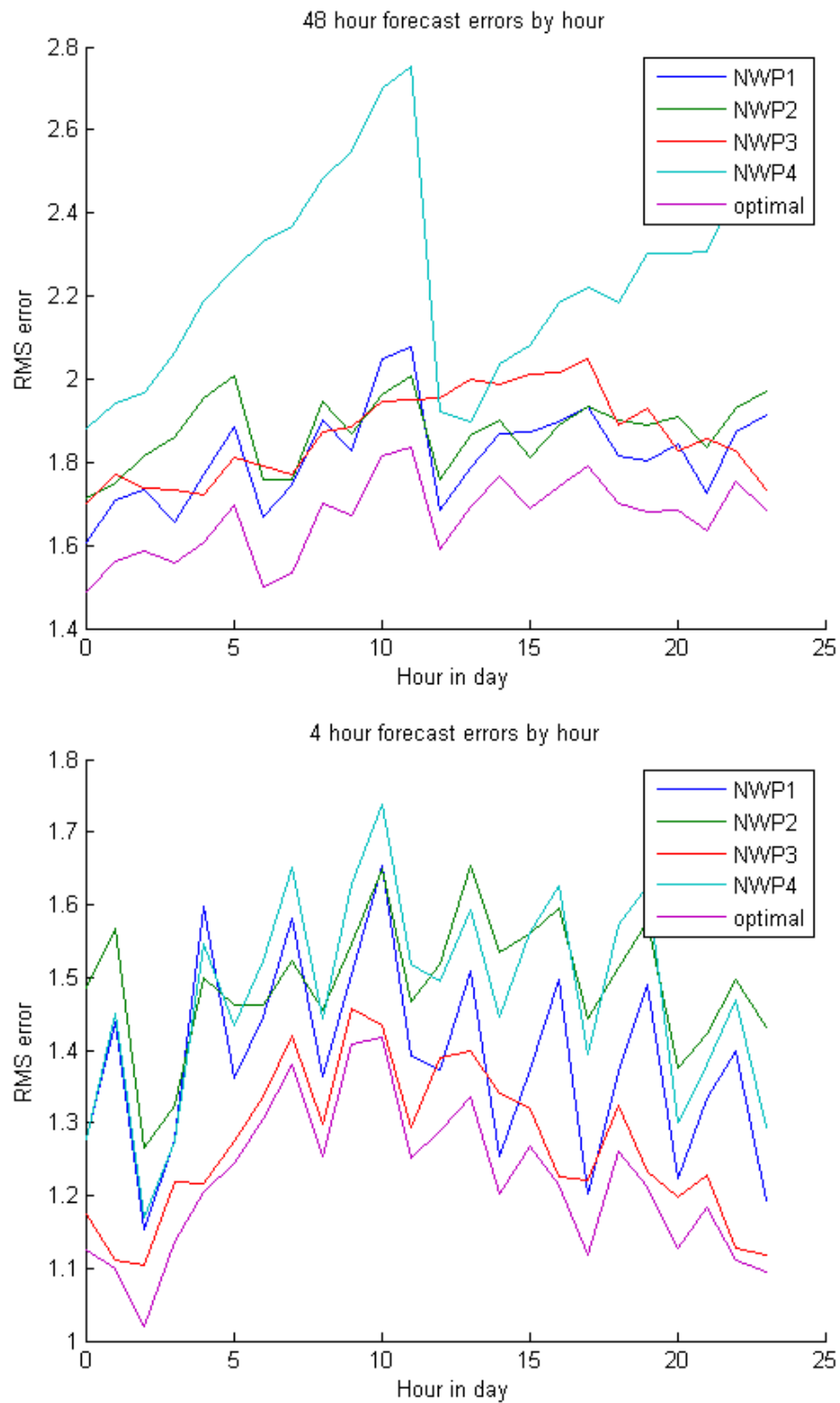


Figure 5: RMS error for (a) 48h forecast and (b) 4h forecast for four individual NWP models and the linear optimised weighting

average of various widths, w :

$$u_i = \frac{1}{w} \sum_{j=i-w}^i v_j \quad i = w + 1 \dots N \quad (3.1)$$

- (3.3) A comparison between the original data and the smoothed data with moving averages of widths of one and two hours respectively are shown in figure 6.

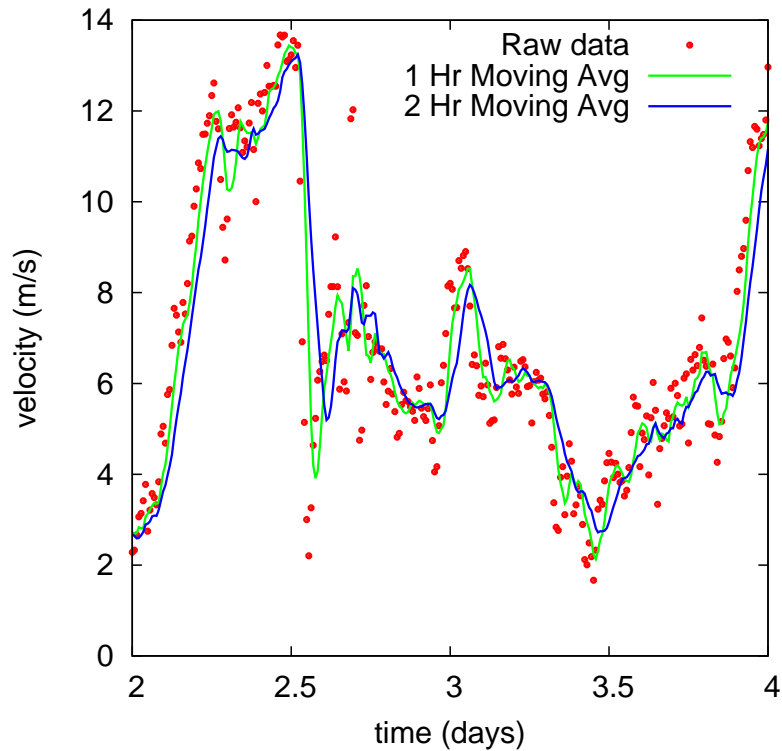


Figure 6: Representative sample of the cleaned, smoothed data for smoothing windows of 1 and 2 hours as compared with the original unsmoothed data.

- (3.4) An autoregressive model of order m (AR(m)) was introduced. This is a linear model in which the next value of in a timeseries is generated from a linear combination of the m previous values plus some noise:

$$x_{i+1} = \sum_{j=1}^m \alpha_j x_{i-j} + \xi_i \quad \xi_i \sim N(0, \sigma^2). \quad (3.2)$$

In this case, the noise is taken to be normally distributed with mean zero and variance σ^2 . This model was then fitted to timeseries obtained by

resampling the smoothed SCADA data at one hour intervals. The intention was to mimic the hourly data used by GH in making their forecasts. The fitting was achieved by solving a standard linear least squares regression on the first two months of SCADA data:

$$\sum_{j=1}^m (\Phi^T \Phi)_{i,j} \alpha_j = \sum_{j=1}^N \Phi_{i,j}^T c_j \quad i = 1 \dots m, \quad (3.3)$$

where

$$\begin{aligned} \Phi_{k,l} &= u_{k-l} & k &= 1 \dots N, \quad l = 1 \dots m \\ c_k &= u_{k+1} & k &= 1 \dots N. \end{aligned}$$

Here N is the length of the timeseries. Some tweaking is obviously required at the ends of the series. The variance of the noise, σ^2 , was obtained from the sum of the squares of the residuals of this fit. The standard deviation of the noise was typically about 1 m/s. In the test runs performed here, we took $m = 12$. That is to say we attempt to forecast using the smoothed data measured during the previous 12 hours.

- (3.5) The predictive skill of the AR(12) model for different levels of smoothing of the raw data is quantified in figure 7. The figure shows the RMS error for forecasts made on the remainder of the SCADA data (i.e. not the data used to fit the model) as a function of the forecast horizon for various levels of smoothing of the data. Two trends are immediately obvious. Firstly, the forecast error increases quite quickly as a function of forecast horizon for all of the timeseries and becomes broadly comparable to random guessing with a forecast horizon of about a day. Here by random guessing, we mean sampling from a normal distribution with the same mean and variance as the observed data. The second trend is that the forecast error increases slightly less quickly as a function of the forecast horizon as the degree of smoothing is increased. This is to be expected since more smoothing means less variation at the expense of less information. To see this, consider that the annual average velocity hardly varies at all and is very predictable but contains no information useful on the timescales of interest here.
- (3.6) The conclusion from this strand of the study is that basic autoregressive models can predict the hourly averaged wind speed to some degree but do

much worse than the real models which incorporate meteorological information.

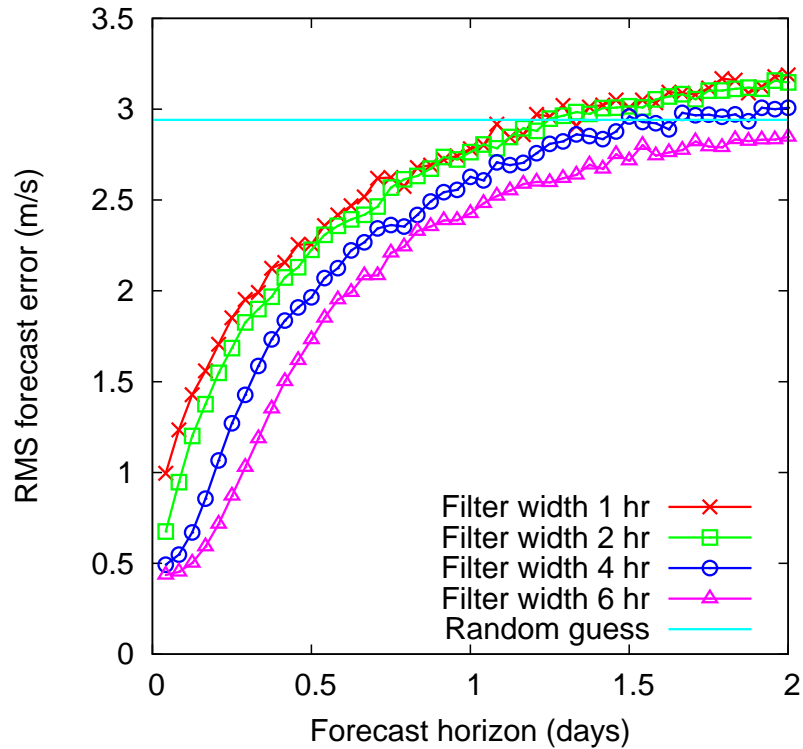


Figure 7: Predictive skill of an AR(12) model for different levels of smoothing.

4 4D-Var Data assimilation

- (4.1) 4D-Variational data assimilation (4D-Var) is a method used to solve a particular kind of inverse problem which can be stated as follows:

Given a set of observations and a numerical model for a dynamical system, find an initial condition for the numerical model that finds the best approximation to the true state of the system, when a priori information for the initial condition is available.

- (4.2) The solution to this problem is found through weighted least squares estimation. This is achieved by minimising the 4D-Var cost function $J : \mathbb{R}^N \rightarrow \mathbb{R}$,

$N \in \mathbb{N}$ with respect to the initial condition for the numerical model, $\mathbf{x}_0 \in \mathbb{R}^N$,

$$\min_{\mathbf{x}_0} J(\mathbf{x}_0).$$

where

$$J(\mathbf{x}_0) = \underbrace{(\mathbf{x}_0 - \mathbf{x}_b)^T B^{-1} (\mathbf{x}_0 - \mathbf{x}_b)}_{:=J_b(\mathbf{x}_0)} + \underbrace{\sum_{l=0}^L [\mathbf{y}_l - \mathcal{H}_l(\mathbf{x}_l)]^T R_l^{-1} [\mathbf{y}_l - \mathcal{H}_l(\mathbf{x}_l)]}_{:=J_o(\mathbf{x}_0)} \quad (4.1)$$

$$\mathbf{x}_{l+1} = \mathcal{M}_{l+1,l}(\mathbf{x}_l) \quad (4.2)$$

(4.3) The result is the optimal initial condition for the numerical model. This is termed the *analysis vector* in the NWP literature and denoted \mathbf{x}_a , (as in e.g. $\nabla J(\mathbf{x}_a) = 0$). The period of time the observations are taken over is known as the *assimilation window*. The observations are not necessarily equally spread in either space or time, so all variables are calculated at the time of each observation.

(4.4) A variable with a subscript l denotes the respective variable at the time of the l th observation of the dynamical system. Specifically:

- $\mathbf{x}_l \in \mathbb{R}^N$ denotes the l th state of the numerical model.
- $\mathcal{M}_{l+1,l} : \mathbb{R}^N \rightarrow \mathbb{R}^N$ denotes the numerical model mapping the l th state of the numerical model, \mathbf{x}_l to its $(l + 1)$ th state, \mathbf{x}_{l+1} .
- N is the number of discretisation points in space in the numerical model.
- $\mathbf{y}_l \in \mathbb{R}^{m_l}$ is the l th observation of the true dynamical system, $m_l \in \mathbb{N} \forall l$.
- m_l is the number of observations in \mathbf{y}_l .
- $\mathbf{x}_b \in \mathbb{R}^N$ is an estimated initial condition for the numerical model used to constrain the initial condition. This is the required a priori information for the method and is termed the *background estimate* in NWP literature.
- $\mathcal{H}_l : \mathbb{R}^N \rightarrow \mathbb{R}^{m_l}$, is the l th *observation operator*. This maps the l th state of the numerical model to the state of the l th observation. As

the observations of the dynamical system are not necessarily at the grid points of the numerical model, the observation operator performs operations such as interpolation to map the state of the numerical model to the same point in space as its corresponding observation for comparison. It may also need to calculate the state of the relevant variables from the state of the numerical model, for comparison with the measured variable in the observation. For example, the l th observation could measure temperature in Fahrenheit whilst the numerical model calculates temperature in Celsius. As a result the observation operator would also need to convert Celsius to Fahrenheit for comparison.

- $B \in \mathbb{R}^{N \times N}$ is the error covariance matrix for the error in the background estimate. This is termed the *background error covariance matrix*.
- $R_l \in \mathbb{R}^{m_l \times m_l}$ is the error covariance matrix for the error in the l th observation and l th observation operator. These are termed the *observation error covariance matrices*.

(4.5) There are several forms of error associated with the variables discussed above. The observations of the true dynamical system all contain errors as for example instrumentation miscalibration. The observation operators introduce representative errors such as interpolation errors. \mathbf{x}_b is an estimated initial condition for the numerical model so also contains errors. These errors are assumed to be uncorrelated and normally distributed. There are also errors present in the numerical model due to inaccurate model equations and numerical implementation. 4D-Var makes the assumption that the model is perfect and doesn't introduce any further errors into the problem [6]. Accounting for model error is currently an active area of research [7].

(4.6) 4D-Var identifies an initial condition for the numerical model that minimises the error between the observations and the results from the numerical model whilst also minimising the error between the background estimate and the initial condition of the numerical model. The former can be seen in $J_o(\mathbf{x}_0)$ and the latter in $J_b(\mathbf{x}_0)$ of (4.1). The process of minimising the error between the initial condition and the background estimate acts to constrain the initial condition to a realistic estimate for the initial condition. The

background error covariance matrix in $J_b(\mathbf{x}_0)$ weights the contribution of the error between \mathbf{x}_b and \mathbf{x}_0 in the cost function according to the accuracy of \mathbf{x}_b , hence attempting to account for the error in the background estimate. Similarly, each observation error covariance matrix weights the contribution of each observation to the cost function. More information can be found in [3, 1].

- (4.7) Once the analysis vector has been calculated, the numerical model can then be run using this initial condition, past the time of the final observation to create a forecast for the system. In real-time forecasting it is important that the real time to create the forecast is less than the forecast window which may be a concern for methods as complex as 4D-Var. As the forecast for the dynamical system is produced, the results of the numerical model diverge from the true state of the dynamical system [5]. As a result, a new initial condition needs to be created periodically to maintain the accuracy of the forecast. With each new set of observations, 4D-Var is performed again and a new forecast is created. This is known as cyclic 4D-Var. In this instance the previous forecast is used to provide the background estimate.
- (4.8) In the case of NWP data the dynamical system is the weather and the numerical model is the forecast model implemented on a spatial mesh on the Earth. 4D-Var is currently used in operational weather centers along with many other methods, such as 3D-Var and ensemble forecasts. 3D-Var is similar to 4D-Var but only uses only one observation in the cost function, from the time of the background estimate. The resulting initial condition is then used to produce a forecast using the numerical model. This process is repeated with each new set of observations from each point in time. As a result, the series of forecasts produces a system which appears discontinuous whilst 4D-Var produces longer forecasts making the forecasts appear less discontinuous and more realistic [1].
- (4.9) In the problem presented, the forecasts provided by the different operational weather forecast centers eg. the Met. Office, each provide a different forecast for the weather at the location of a wind farm. These forecasts are made on grids which are large in comparison to the scale of the wind farm. For example, the smallest grid resolution offered by the Met. Office over the UK is approximately 1.5km. These forecasts are not tailored to

the locations of the wind farms, so do not always provide the best forecast. However, the forecast is a realistic estimate as to the weather at the location of the wind farm. In this way it can be used as the a priori information required to constrain any local application of 4D-Var ie: it can be used as the background estimate for localised forecasting at the wind farm using 4D-Var. The forecasts received from the operational weather forecast centers can be combined optimally as discussed in Section 2, using (2.1), to produce a good background estimate for localised 4D-Var. A background error covariance matrix can be created from knowledge of the statistics of the data.

(4.10) The observations for the localised 4D-Var would be provided by the SCADA data. Observation error covariance matrices can be created from analysis of the statistics of the errors in the observations. A numerical model for the wind speeds would also be required.

(4.11) The ARMA model suggested in Section 3 is trained using 2 months of SCADA data to produce the coefficients a_1, \dots, a_m, ξ , where $m \in \mathbb{N}$. These remain fixed within the model. The model requires m consecutive wind speeds in order to estimate the next wind speed from the model. Let u_n denote the n th wind speed of the model, then

$$u_n = \sum_{j=1}^m a_j u_{n-j} + \xi_{n+j} \quad (4.3)$$

As a result the effective initial conditions in this situation are the m previous wind speeds. Let $n = 0$ denote the time of the first observation in the application of 4D-Var. Then the optimal initial condition to be found is $\mathbf{x}_0 \in \mathbb{R}^m$ such that $\mathbf{x}_0 = [u_{-1}, \dots, u_{-m}]^T$. Each observation $\mathbf{y}_l \in \mathbb{R}^m$ would contain the m previous wind speed observations from the SCADA data, ie: $\mathbf{y}_l = [u_{l-1}^{SCADA}, \dots, u_{l-m}^{SCADA}]^T$. The background estimate would also be of a similar form to these. As the data used to train the ARMA model was created by smoothing the SCADA data and sampling it at equal intervals, the ARMA model requires data sampled at these equal intervals. As a result the background estimate and SCADA observations will also need to be interpolated to these equally spaced points in time to provide the required data for the 4D-Var process.

- (4.12) Once the optimal m wind speeds have been calculated, these can then be used to generate a local forecast for the wind speeds at the wind farm, using the ARMA model. The difficulty with using an ARMA model is that the model needs to be re-trained on previous data to create the model variables, for each new application of the data assimilation process. This also adds extra time to the forecasting process. The length of this extra time depends on the number of model parameters and the size of the training data. A balance between the processing time and the accuracy of the forecast would need to be found experimental to identify the best size for the training data set. The background states also need to be identified from the forecasts provided by the operational forecast centers. Depending on the length of time between each observation used in the ARMA model, this data may need to be interpolated in time as these forecasts may be sparse in time by comparison.

5 Artificial neural networks

- (5.1) Artificial Neural Networks (ANN) with radial basis functions were employed to try and predict the wind speed for different horizons (H). Two basic methods were established: using several past measured values (SCADA data) to predict the wind speed H hours later and using the four available Numerical Weather Prediction (NWP) data to predict the wind speed H hours later. The results are compared to the most obvious prediction, that is, the estimation of the naive predictor (also called persistence), which takes the wind speed in H hours to be the same as it is at the time of making the prediction. For this task generalised regression neural networks were used.

5.1 Generalised Regression Neural Networks

- (5.2) The ANN was simulated in MATLAB using `newgrnn`, which creates a New Generalised Regression Neural Network (two-layer network) like the one presented in figure 8. The first layer takes P as the input which is a vector of length R , the total number of input - target pairs is Q . It has `radbas` neurons (see figure 9) and calculates weighted inputs with Euclidean distance weight function (`dist`) and net inputs with `netprod`. The second layer has linear transfer function neurons (`purelin`, see figure 9) and calculates weighted input with normalised dot product weight function (`normprod`) and net

Generalised Regression Neural Network

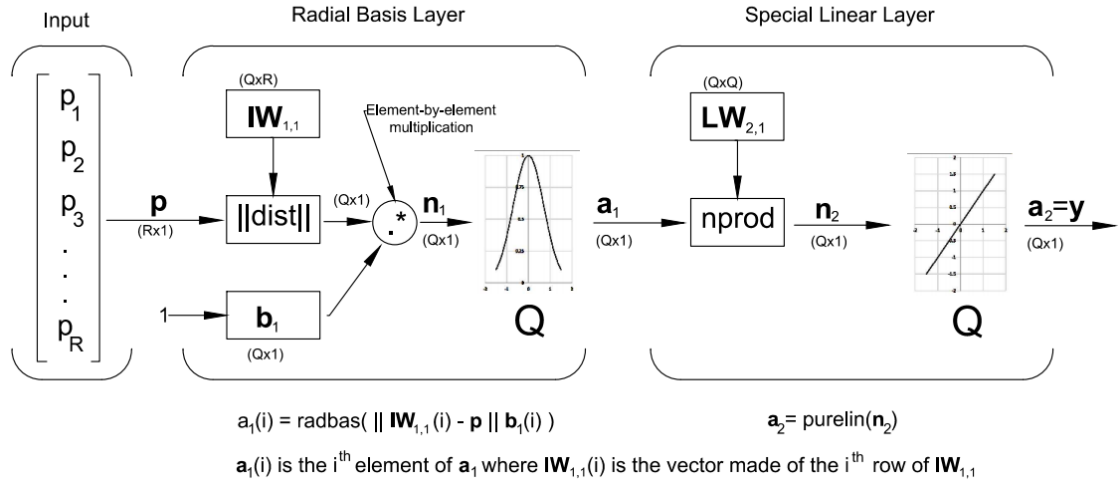


Figure 8: Architecture of the Generalised Regression Neural Network

inputs with sum net input function (`netsum`). The structure of the neural network is shown in figure 8.

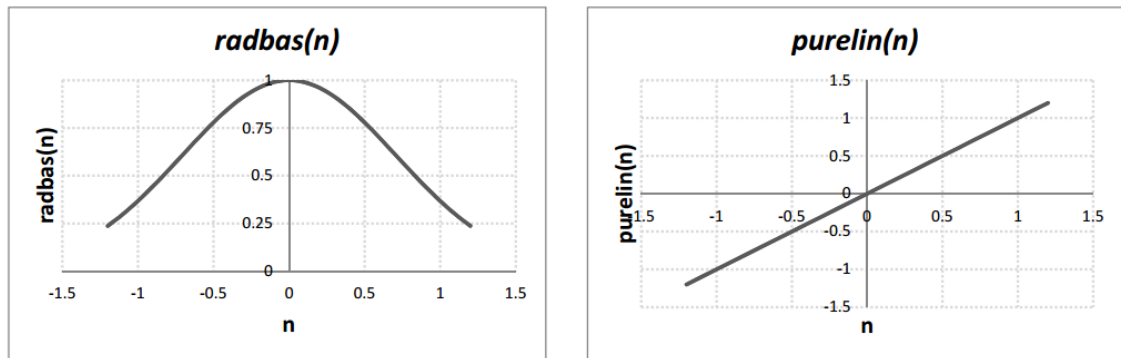


Figure 9: The `radbas(n)` (left) and `purelin(n)` (right) functions.

5.2 ANN prediction from SCADA data

- (5.3) Based on previous results of auto-regressive methods presented in section 1, SCADA data were assumed to be useful only on a short horizon with the maximum taken to be about 8 hours. The neural network used the smoothed wind speed data (with zero values removed, etc) as input, with

hourly average wind speeds formed from the available 10 minutes resolution data. The predictor aims to predict the wind speed H hours later based on several previous hourly average wind speeds, the number of past data R was varied between 1 and 96 (1 hour to 4 days), the input vector P has a size of $(R \times 1)$. The ANN needed to be trained on a high number of data values (Q), in the order of magnitude of 1000 to 10000. The training process used Q vectors of length R as the input, the targets $T^{1 \times 1}$ were the measured wind speed values H hours later; the Q input vectors $P^{R \times 1}$ had Q target values $T^{1 \times 1}$. Figure 10 shows the input and target for $H=5$, $Q=3$ and $R=4$.

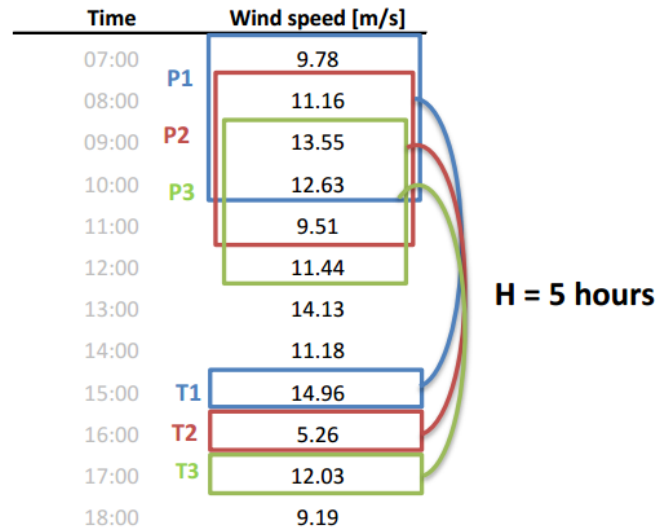


Figure 10: GRRN for SCADA values: P1,P2,P3 are the inputs, T1,T2,T3 are the targets. Example: $Q=3$, $R=4$, $H=5$.

- (5.4) The sensitivity of the prediction accuracy to the number of inputs (Q) was tested and it was found that the precision does not increase above several thousand inputs, therefore the final testing was carried out with 10000 training data. The prediction accuracy of the neural network was tested for various numbers of past data used (R), and it was found that using data of more than the last 12 hours decreases the performance of the network (see figure 11). To evaluate the performance of the neural network, the RMS error of the simulation was compared to the RMS error of the persistence estimator. It was found that between about 4 and 8 hours horizon the result of the neural network prediction using 2 to 8 previous values shows a slight (no more than 5%) improvement compared to the

persistence prediction.

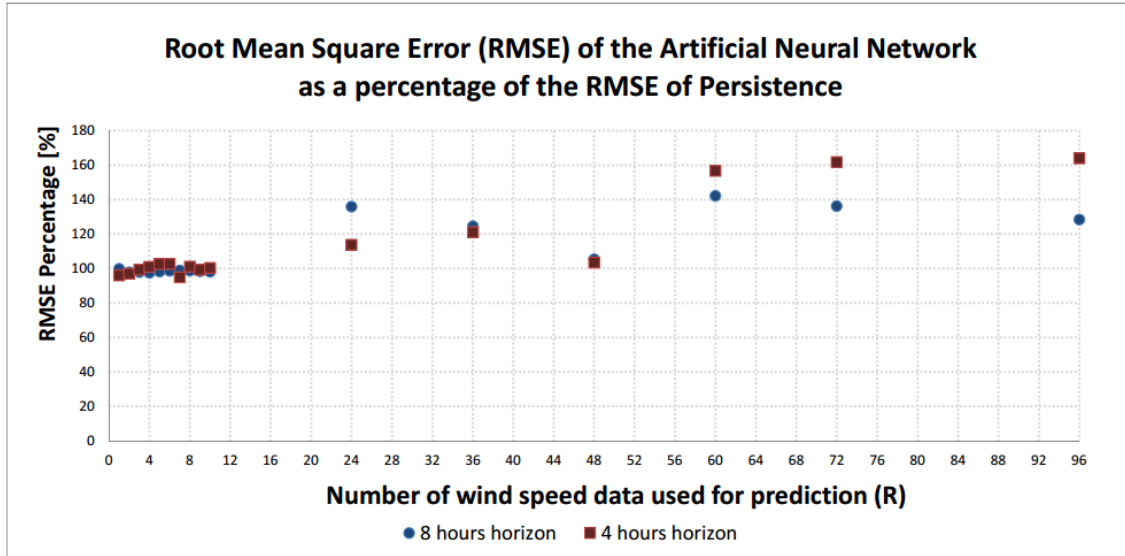


Figure 11: RMS error of the neural network using SCADA values as percentage of the RMS error of the persistence estimation for H=4 and H=8 hours horizons.

5.3 ANN prediction from Numerical Weather Prediction data

- (5.5) Prediction for the longer term (more than 12 hours) was made by using the four available NWP data as input for the generalised regression neural network. The architecture was the same as the one presented above. The input vector $P^{R \times 1}$ is a 4 element vector, the targets $T^{1 \times 1}$ are the measured wind speed values (SCADA) at the site at the predicted time. The network was trained on Q number of data. Figure 12 shows the process for Q=3, R=4 and H=30 hours). The available data to train the network was limited: the raw data required a significant amount of post-processing before it could be used as network input. An input file was prepared such that it contained 365 lines of data for every day of the 1 year worth of data available. For every day the predictions of all four NWP models available at a given time of the day (e.g. 9am) were taken, and the predictions of the wind speed 30 hours later (e.g. 3pm the next day) were stored. This limitation meant that the network could be trained only on a short dataset, not more than about 300 input - target pairs.

Time of making prediction		NWP1	NWP2	NWP3	NWP4	Predicted time	Measured value	
09:00, Monday	P1	11.84	10.59	9.25	5.01	15:00, Tuesday	7.01	T1
09:00, Tuesday	P2	10.54	12.57	12.47	12.72	15:00, Wednesday	13.92	T2
09:00, Wednesday	P3	11.51	15.16	14.46	14.33	15:00, Thursday	16.33	T3
09:00, Thursday		7.70	3.90	2.42	3.97	15:00, Friday	2.29	
09:00, Friday		8.49	10.27	9.89	9.76	15:00, Saturday	9.03	
09:00, Saturday		14.58	15.03	15.00	15.12	15:00, Sunday	14.79	

Figure 12: GRRN for NWP values. Example: $Q=3$, $R=4$, $H=30$.

- (5.6) Due to the long horizon taken in this simulation, the comparison to persistence is no longer a suitable method of evaluation (since its RMS error is comparable to the standard deviation of the wind speed), therefore the results are compared to the prediction made by taking the average of the four NWP models. For large datasets of predictions it was found that the RMS error of the average of the four NWP models was 1.5767 m/s. In comparison, the neural network, after training on a few hundred data, produced predictions with RMS error of 1.3938 m/s. This is a significant 12% improvement to the NWP average. (The standard deviation of the wind speed was 2.271 m/s.)
- (5.7) It is important to note that the accuracy of the predictions shows an increase with higher amounts of training data, however, the increase is getting less and less significant above about 150 training inputs. Training with more diverse data (i.e predictions of different hours of the day, and predictions from multiple years) and with a significantly higher number of data would likely increase the performance of the neural network.

5.4 Remarks and possible future work

- (5.8) The short term prediction with neural networks with a horizon of less than 12 hours using SCADA data provided a slight improvement over the simple naive estimator. Other methods (e.g. ARMA) provided better results, therefore application of neural networks for short term prediction by using SCADA data alone does not seem practical.

- (5.9) Longer term predictions (12-36 hours) were made using NWP data, and an RMS error reduction of 12% was achieved on a horizon of 30 hours compared to the average of the NWP data. The network was trained on a small amount of data, each of them from the same hour of the day. More diverse data and a higher number of input-target pairs would likely improve the performance of the GRNN.
- (5.10) From the achieved results it seems advisable to try and combine the inputs from SCADA data and the NWP predictions on the short term and optimise the performance by considering the usability of the methods on different horizons. Combining the ANN's with an ARMA model would likely give optimal results for both long and short term predictions.

6 Kernel dressing

- (6.1) Using the NWP point forecasts of the wind speed provided, we can produce probabilistic forecasts that take account of the uncertainty around them. We show how to build such forecasts and suggest ideas as to how they could be improved.
- (6.2) Suppose we wanted to predict the wind speed in 24 hours time. Whilst any forecast has some uncertainty, we would expect to do reasonably well running a model that uses some insight into the likely evolution of the weather conditions from now until tomorrow. Now suppose we wanted to predict the wind speed exactly a year from now. Running a model that evolves today's conditions for a whole year would give us a poor estimate of the actual outcome, and any resemblance is simply from coincidence. In reality, the best we can do without specific forecast information is to look at some estimate of the long term distribution of wind speeds at that particular point in time, so we might estimate the distribution from observations of wind speed at this time of the day for the last 10 years. Alternatively, we could look at the distribution of wind speeds just in the particular month the day we are predicting the wind for falls. We may even look at wind speed for the specific date of the year we are trying to predict over say the last 100 years (although clearly this isn't possible for wind farms). We call these distributions 'climatology'. Since we can always (when available) use the climatology as a simple probabilistic forecast, it provides a lower bound

on how skillful we expect any model predictions for a specific day to be. A model prediction that tends to give a worse forecast than climatology could give us is of very little practical use. For this reason, we will always score models relative to climatology.

- (6.3) As we have discussed, the climatological distribution can take many forms. Here, we discuss a few possible approaches and settle on one which we use in the rest of this section.

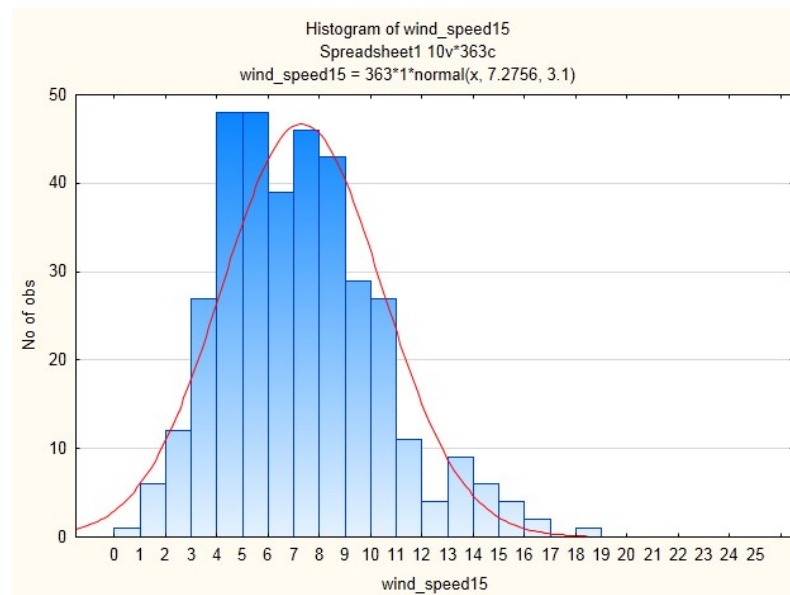


Figure 13: Climatological distribution over the entire year.

- (6.4) Figure 13 shows a fit of the PDF of a normal distribution to the climatological data from an entire year. This describes the distribution of windspeeds over the entire year of data we are considering. Were we just making predictions of the wind speed in a particular month, we may want to use an estimate based purely on the climatology for that month as shown in figure 14 for January or figure 15 for July. Ideally we would use the climatology that is most specific to the forecasts we are considering however this is always balanced with availability of relevant data. In this report we use the normal distribution obtained from an entire year's data.
- (6.5) An additional consideration is the choice distribution to be used in modelling the climatology. We have used a Gaussian distribution as a first step due

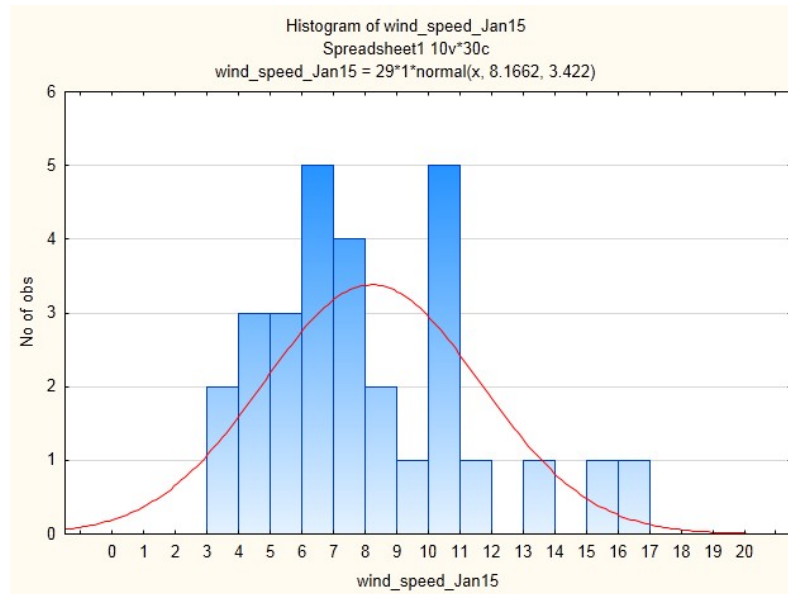


Figure 14: Climatological distribution just using data from January.

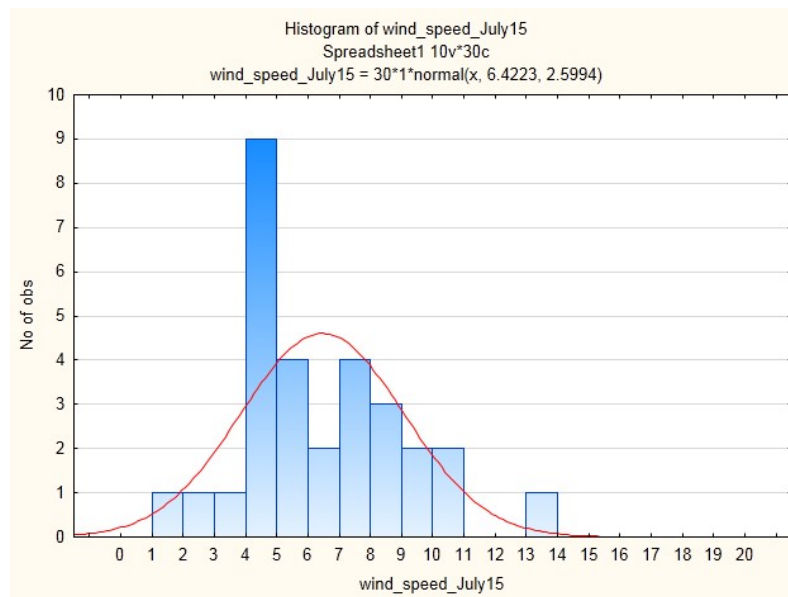


Figure 15: Climatological distribution just using data from July.

to time constraints, however due to the complex nature of windspeed as a variable it is likely that some other distribution would perform better.

- (6.6) In order to choose between the various models that we will introduce in this section, we need a way of comparing the effectiveness. The particular

method we use is the *Ignorance Score*. First introduced by IJ Good in 1952 [4], it is given by $IGN = -\log_2 p$ where p is the amount of probability placed on the eventual outcome. This particular skill score has desirable properties for this kind of forecasting. For reasons discussed above, all ignorance scores in this report are given relative to climatology, that is $IGN_{rel} = IGN(mod) - IGN(clim)$.

- (6.7) It is often beneficial to ‘blend’ a model with the Climatological distribution. The reason this can be useful is that the climatology generally takes into account all possible values the verification can take, whereas a model might have a bias or be too narrow in its coverage. To do this, we simply take a weighted average of the model and the climatology in the form:

$$P(y) = \alpha P_{mod}(y) + (1 - \alpha) P_{clim}(y) \quad (6.1)$$

where $P_{mod}(y)$ is the probabilistic forecast from the model and $P_{clim}(y)$ is an estimate of the distribution of the climatology. $0 < \alpha < 1$ is a parameter that can be found by minimising the mean ignorance over a training set (forecasts and verifications from the past).

- (6.8) We introduce a number of simple probabilistic models for wind speed and compare their skill using relative ignorance. All of these results correspond to the most recent forecast available at 9am for 3pm the following day.

6.1 Running mean and variance normal distribution model

- (6.9) Our first model is very simple. A probabilistic forecast is made using a normal distribution with mean taken to be the average wind speed at 3pm over the previous 5 days and the variance taken to be the variance of the wind speed over the previous 30 days, i.e.

$$\text{Model 1 - } P(y) = N(\text{mean}(x_{t-1}, \dots, x_{t-5}), \text{var}(x_{t-1}, \dots, x_{t-30})).$$

- (6.10) We consider two cases, the model without blending ($\alpha = 1$) and the model blended with climatology (with optimal α with respect to the ignorance). Since this model is very simplistic, we have no reason to expect it to perform well, it is however useful for illustrative purposes in that using this model on its own actually gives a positive relative ignorance, i.e. it does worse than climatology. This is useful to note because realising this simple fact

enables us to disregard the model for any useful purposes. However, when we blend the model with climatology, we find a slightly negative relative ignorance albeit very close to 0. We see here, the benefits of blending with climatology.

α	Relative Ignorance
1	0.38
0.3	-0.02

Table 2: Relative ignorance scores for running mean and variance model.

6.2 Individual Kernel Dressed Model forecasts

(6.11) For this model, we use the NWP data point forecasts provided. We use a method called Kernel dressing which turns a set of points into a probability distribution by replacing each one with some probability distribution called a Kernel. The estimated PDF is then found by averaging the density of the kernels at each point. In this case, where we have a single point forecast this simply reduces to replacing the single point with a probability distribution. Commonly, and this is what we do here, a Gaussian Kernel is used. For this model, we assume that we have a learning set of forecasts and corresponding verifications from which we can ‘tune’ our probabilistic forecast (although due to lack of data to work with, this has been done in sample). The mean of the distribution is taken to be the point forecast itself with a bias correction found from the learning set ($\mu_i = \bar{f}_i - \bar{y}_i$ over the learning set) and the standard deviation is taken as the standard deviation of the error also found from the learning set ($\sigma_i = std(f_i - y_i)$ also over the learning set). Each probabilistic forecast is blended with climatology with the value of α optimised with respect to the ignorance score. Formally, each model is given by:

$$P(y) = N(f_i - \mu_i, \sigma_i^2) \quad (6.2)$$

where f_i denotes the point forecast for NWP model i , μ_i is an offset parameter designed to correct the mean of the distribution and σ_i is the standard deviation which is of course also a parameter.

(6.12) Here we find that the model using NWP1 forecasts performs the best followed by the model using NWP2 forecasts. All of the forecasts give a

negative relative ignorance indicating that we improve on climatology in all cases.

Forecast	NWP1	NWP2	NWP3	NWP4
Relative ignorance	-0.93	-0.88	-0.67	-0.79

Table 3: Relative ignorance scores from using kernel dressing with each of the different NWP data sources.

6.3 Possible future work

(6.13) In this section we have introduced a number of very simple models to create probabilistic forecasts from point forecasts. Due to time constraints we only considered normal distributions which may be unrealistic. Given more time it would be beneficial to consider distributions that describe the data better. Another step that would be highly beneficial in improving such forecasts would be to use ensemble forecasts. Advanced methods exist that convert ensembles to probability distributions with little assumption about the properties of such distributions (See for example [2]). We would expect such methods to perform very well for data of this kind.

7 Conclusions

(7.1) The optimal linear combination of the NWP forecasts was used as a benchmark for more advanced methods and resulted in RMS errors of 1.28-1.68 ms^{-1} for prediction windows of 4-48 hours. The 30 hour RMS error of 1.46 ms^{-1} found for this method is slightly poorer than the corresponding 30 hour RMS error of 1.39 ms^{-1} found using artificial neural networks. It is possible that the artificial neural network does not add much predictive value over a simple linear combination of forecasts although it is likely that the artificial neural networks would perform better given a larger training data set. Due to its complexity the 4D-Var method was not fully implemented during the timeframe so we do not have results to compare with the other forecasting methods. For shorter prediction windows ($\approx 0-6$ hours) the ARMA model based only on the SCADA data appeared to give the smallest RMS error although the comparison is with respect to smoothed data so it is unclear how exactly this compares with the other methods. The output of the kernel dressing method is a distribution rather than a point estimate.

Consequently its performance was measured in terms of relative ignorance scores which are not directly comparable to the RMS errors used for the other methods. It is unclear exactly how this compares with, for example, the optimal linear combination.

- (7.2) While the methods considered vary significantly in their complexity each demonstrated some predictive value. However we have been unable to conclusively show that any of the methods provides a significant improvement over the simplest method which involves taking the (optimal) linear combination of the available NWP forecasts at the time of interest.

Bibliography

- [1] F. BOUTTIER AND P. COURTIER, *Data assimilation concepts and methods*, Meteorological Training Course Lecture Series, (1999).
- [2] J. BRÖCKER AND L. A. SMITH, *From ensemble forecasts to predictive distributions*, Tellus Series A, 60 (2008), pp. 663–678.
- [3] R. DALEY, *Atmospheric Data Analysis*, Cambridge Atmospheric and Space Science Series, Cambridge University Press, Cambridge, UK, 1st ed., 1999.
- [4] I. GOOD, *Rational decisions*, Journal of the Royal Statistical Society, 14 (1952), pp. 107–114.
- [5] E. HÓLM, *Lecture notes on assimilation algorithms*, Meteorological Training Course Lecture Series, (2003).
- [6] A. LORENC, *Analysis methods for numerical weather prediction*, Quarterly Journal of the Royal Meteorological Society, 112 (1986), pp. 1177–1194.
- [7] N. NICHOLS, *Treating model error in 3-D and 4-D data assimilation*, in Data Assimilation for the Earth System, R. Swinbank, V. Shutyaev, and W. Lahoz, eds., vol. 26 of NATO science series, Springer Netherlands, 2003, pp. 127–135.